Journal of Computer-Aided Molecular Design, 10 (1996) 479–489
ESCOM

J-CAMD 356

The agonistic binding site at the histamine H_2 receptor. II. Theoretical investigations of histamine binding to receptor models of the seven α-helical transmembrane domain

Paul H.J. Nederkoorn, Erna M. van Gelder, Gabriëlle M. Donné-Op den Kelder and Henk Timmerman*

Department of Pharmacochemistry, Leiden/Amsterdam Center for Drug Research (LACDR), Vrije Universiteit, De Boelelaan 1083, 1081 HV Amsterdam, The Netherlands

Received 26 February 1996
Accepted 28 May 1996

Keywords: G-protein-coupled receptor; Hartree–Fock calculations; Histamine H_2 receptor; Molecular mechanics; Receptor models

Summary

In the first part (pp. 461–478 in this issue) of this study regarding the histamine H_2 receptor agonistic binding site, the best possible interactions of histamine with an α-helical oligopeptide, mimicking a part of the fifth transmembrane α-helical domain (TM5) of the histamine H_2 receptor, were considered. It was established that histamine can only bind via two H-bonds with a pure α-helical TM5, when the binding site consists of Tyr^{182}/Asp^{186} and not of the Asp^{186}/Thr^{190} couple. In this second part, two particular three-dimensional models of G-protein-coupled receptors previously reported in the literature are compared in relation to agonist binding at the histamine H_2 receptor. The differences between these two receptor models are discussed in relation to the general benefits and limitations of such receptor models. Also the pros and cons of simplifying receptor models to a relatively easy-to-deal-with oligopeptide for mimicking agonistic binding to an agonistic binding site are addressed. Within complete receptor models, the simultaneous interaction of histamine with both TM3 and TM5 can be analysed. The earlier suggested three-point interaction of histamine with the histamine H_2 receptor can be explored. Our results demonstrate that a three-point interaction cannot be established for the $Asp^{98}/Asp^{186}/Thr^{190}$ binding site in either of the investigated receptor models, whereas histamine can form three H-bonds in case the agonistic binding site is constituted by the $Asp^{98}/Tyr^{182}/Asp^{186}$ triplet. Furthermore, this latter triplet is seen to be able to accommodate a series of substituted histamine analogues with known histamine H_2 agonistic activity as well.

Introduction

Pros and cons of 3D G-protein-coupled receptor models

The three-dimensional (3D) structure of one α-helix is well defined, but, in contrast, the positioning of the seven transmembrane α-helices of G-protein-coupled receptors (GPCRs) in relation to each other is less profound. This is illustrated by the differences in 3D protein models reported for particular GPCRs, which are all based on the experimentally determined 3D structure of bacteriorhodopsin (BR) (e.g. Refs. 1–4, and references cited therein). Before any experimental 3D data on GPCRs became available, these receptors were believed to possess a membrane-bound domain similar to the one observed for BR, which was the first membrane-bound protein in which the presence of a seven antiparallel α-helical motif was established experimentally. Although after some time, also the GPCR rhodopsin was experimentally shown to contain a seven α-helical motif [5] – indicating that this feature is probably common to all GPCRs – there are still several uncertainties in the aforementioned GPCR models based on BR. These uncertainties mainly stem from a very low primary sequence homology between BR and GPCRs, and in addition from the very low resolution (≈ 9 Å) electron diffraction density maps from which the structures for BR and rhodopsin have been inferred. Further-

*To whom correspondence should be addressed.

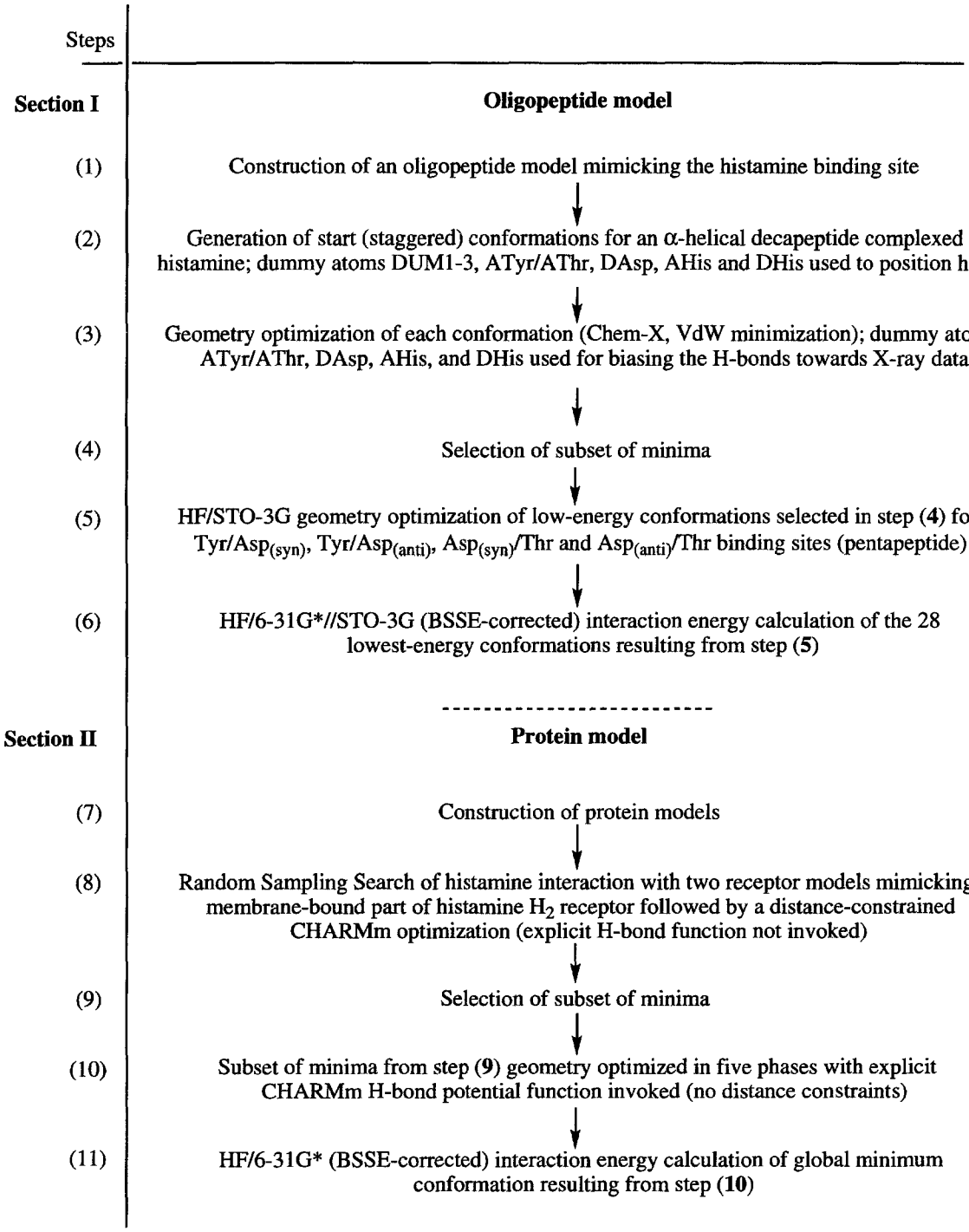

Fig. 1. Flow chart of the overall strategy to approach histamine binding to its binding sites at TM3 and TM5 of the histamine H_2 receptor.

more, the density maps for BR and bovine rhodopsin differ [4–7]. These differences have, however, been ascribed to the fact that the electron diffraction images were made under a slightly different angle of 15° [3,4]. In spite of the aforementioned uncertainties, several models have been developed which aim at a correct description of the relative orientation of the seven transmembrane α-helices in GPCRs. These models are all based on information derived from: (i) hydrophobicity plots of GPCR multialignments which indicate the location of hydrophobic, presumably transmembrane, domains; (ii) the presumed relation between the α-helical positions in BR and GPCRs; and (iii) the presumed orientation of both polar, conserved, as well as ligand-binding residues towards the inner core of the receptor. However, the largely varying width of the hydrophobic domains in GPCRs and the low-sequence homology with BR still make several alignments with BR possible and can therefore lead to at

least questionable GPCR homology models. Thus, although the multiple-sequence alignment of GPCRs itself is uniquely defined (e.g. Ref. 1), the alignment of a GPCR with its template for homology building, BR, is not. This explains that also for the histamine H_2 receptor a number of models have been reported (e.g. Refs. 1, 3 and 4, and references cited therein) in which the relative position of the α-helices varies; this variation affects of course the binding site for small molecules, both agonists and antagonists. Because of these uncertainties, we have first (Part I) chosen to investigate the binding of the histamine heterocycle to two putative binding sites on a separate α-helix, since only then the relative positions of amino acids can be defined in a unique manner. This section (Section II, Fig. 1) focuses on the influence of selecting a particular BR/GPCR alignment on the constitution of the most likely agonistic binding site for the histamine H_2 receptor.

The effect of choosing a particular alignment on the relative position of α-helices in protein models for the histamine H_2 receptor can be illustrated by investigating the binding of histamine in different models. For this purpose, we have selected two models (Fig. 1, step **7**): one based on a thorough sequence alignment reported by Oliveira et al. [1] (indicated as Model A), and another which incorporates a very attractive activation mechanism, in which receptor activation theoretically results in the delivery of at least one proton intracellularly per agonist bound [3] (indicated as Model B). Since it is generally accepted that histamine binds at TM3 and TM5 (e.g. Ref. 1), we focused on these two α-helices. Within Model B [3], TM3 starts at Ile^{93} and ends with Ala^{119}; within Model A [1] TM3 starts at Phe^{90} and ends with Arg^{116} (amino acid numbering for both human and canine histamine H_2 receptors [8]). In both models, TM5 starts at Tyr^{182} and ends with Tyr^{202}. Hence, TM5 is the same in both models, but TM3 differs, resulting in different relative orientations of the amino acids of these two helices. The development of these models enables a comparison with the theoretical results obtained from the α-helical model system described in Part I. Although binding of the histamine heterocycle to specific sites on TM5 might be allowed when TM5 is studied separately, this binding can be influenced by the presence of amino acids from other helices despite the flexibility of the side chains. Also a simultaneous three-point interaction (Refs. 9–14; vide infra) between histamine and the protein can possibly not be established in the transmembrane protein models. Consequently, such differences may influence the results obtained with the separate protein models.

Although GPCR homology models definitely have several pitfalls, the simultaneous interaction of ligands with more than one helix can only be addressed when all possibly interacting amino acids are present. This makes the use of receptor models indispensable. In the model derived in Part I, the histamine side chain is pointing from TM5 towards the central cavity, but its explicit interaction with Asp^{98} of TM3 could not be examined. Within transmembrane protein models, the relatively strong interaction between the positively charged side chain of histamine and the negatively charged Asp^{98} from TM3 might prevent that the optimal interaction between the histamine imidazole ring and two hydrogen-bonding residues as found for the TM5 model system (Part I) can be established.

Since a three-point interaction (protein models) limits the positional freedom of histamine within putative binding sites more than a two-point interaction (TM5 model system, Part I), the flexibilities of the interacting amino acids do not have to be considered to their full extent. This allows for the application of a more accurate force field and optimization of the protein backbone as well. The additional flexibility introduced into the backbone by glycine residues (Gly^{183} and Gly^{187}) and its effect on histamine binding can therefore be studied. Studies on the TM5 model system (Part I) revealed that the histamine ring system cannot interact simultaneously with Asp^{186} and Thr^{190}. However, the results could have been influenced by the obligation to keep the α-helical backbone fixed. Therefore, within protein models, two putative binding sites for histamine on TM5 (the Tyr/Asp and Asp/Thr couple from Part I) were investigated again.

Series of substituted agonists

A number of known histamine H_2 receptor agonists are substituted at the 4/5-position (cf. compound **3**, Table 1) and/or at the 2-position of the heterocycle (cf. compounds **2** and **4**, Table 1; e.g. Refs. 10 and 11). Therefore, we also investigated whether these substitutions are tolerated within the two putative binding sites of the protein models.

Methods

Overall strategy to approach histamine binding to its putative binding sites within two receptor models

The oligopeptide model system mimicking a part of TM5 was addressed in Part I (steps **1**–**6**, Fig. 1). Section II consists of the following steps: first, the protein models were built (step **7**) followed by a limited conformational analysis with subsequent geometry optimization of the protein models complexed with histamine (step **8**). A subset of lowest energy minima was selected (step **9**) and further optimized with an explicit H-bond potential function invoked (step **10**). Finally, the resulting global minima for both the Tyr/Asp and Asp/Thr binding sites were ab initio analysed (step **11**). The subsequent steps of Section II and the computational methods used are now discussed in detail.

TABLE 1
BIOLOGICAL ACTIVITIES AND TITRATION DATA FOR HISTAMINE AND SUBSTITUTED HISTAMINES

No.	Compound	pK_d [a]	n	pD_2 [b]	α [c]	n	log K_1 [d]	log K_2 [e]	n	Mol % [f] monocation at pH = 7.4
1	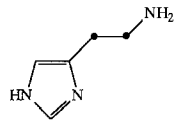	4.16 ± 0.08	3	6.14 ± 0.04	1.00	22	9.32 ± 0.14	5.93 ± 0.14	3	95.6
2	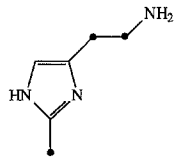	3.62 ± 0.11	2	4.57 ± 0.09	0.93 ± 0.03	2	9.40 ± 0.02	6.83 ± 0.01	3	78.2
3	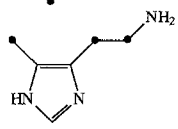	3.60 ± 0.10	4	5.70 ± 0.05	1.02 ± 0.04	2	9.25 ± 0.07	6.48 ± 0.01	3	88.2
4	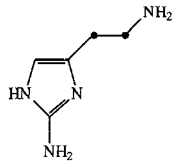	3.30 ± 0.03	3	5.26 ± 0.02	0.85 ± 0.02	3	9.45 ± 0.02	7.34 ± 0.01	3	53.2

[a] Binding to guinea pig *cortex*.
[b] Histamine H2-receptor activity on isolated guinea pig right *atrium* (chronotropic effect).
[c] Intrinsic activity.
[d] Proton association constant of the side chain.
[e] Proton association constant of the heteroaromatic nucleus.
[f] Calculated mole fractions based on log K_1 and log K_2.
All the values given are mean values ± SEM of n independently performed experiments.

Transmembrane protein model systems (Fig. 1, Section II)

Construction of the protein models (Fig. 1, step 7)

Three-dimensional coordinates for the histamine H_2 receptor model as described by Oliveira et al. [1] were directly obtained from the authors [2] (Model A). Model B for the histamine H_2 receptor was obtained via homology building in QUANTA 4.0 [15] using the human β_1 adrenergic receptor model as reported by Timms et al. [3] as a template. In both the models, histamine binding was investigated. Histamine was either positioned in between Asp^{98} (TM3) and the Tyr^{182}/Asp^{186} couple (TM5) or in between Asp^{98} (TM3) and Asp^{186}/Thr^{190} (TM5). The main determinants for the interaction between histamine and the histamine H_2 receptor were thus assumed to be the earlier-mentioned three hydrogen bonds [9–14], one of them having an ionic character (Asp^{98} interacting with the positively charged side-chain amino group of histamine). The CHARMm [15,16] force field was used throughout Section II (steps **8–10**). Although this force field is more accurate than the minimal vdW force field used in Section I [17], again no fully adequate H-bond functions are present, as described below.

CHARMm [15,16] Chem-X [17] – originally developed for smaller molecules – has been applied to the oligopeptide model system (Part I, steps **1–3**, Fig. 1), since dummy atoms and restraint forces can easily be defined within this programme. Also a minimal vdW force field is available, which makes a fast geometry optimization of molecular structures possible. Because the CHARMm force field has mainly been developed for proteins, we judged it to be more suitable for the investigations in this section (steps **8–10**). The CHARMm force field [15,16] offers an explicit term to describe the H-bond between a hydrogen donor (D) and an acceptor (A):

$$E_{hb} = [\{(A'/r^i_{AD}) - (B'/r^j_{AD})\} \cos^m(\theta_{A\text{-}H\text{-}D}) \cos^n(\theta_{AA\text{-}A\text{-}H}) \, sw(r^2_{AD}, r^2_{on}, r^2_{off}) \, sw(\theta^2_{A\text{-}H\text{-}D}, \theta^2_{on}, \theta^2_{off})] \quad (1)$$

Here, i and j are positive integers and are available as parameters for the hydrogen bond under consideration. (N.B.: In earlier CHARMm releases, i and j were fixed at 12 and 10, respectively.) A' and B' are also parameters depending on the A-D pair, with r_{AD} the distance between the hydrogen donor and acceptor. $\theta_{A\text{-}H\text{-}D}$ is the angle between the acceptor, hydrogen and donor, whereas $\theta_{AA\text{-}A\text{-}H}$ is the angle between the acceptor antecedent, acceptor and accepted hydrogen. Depending on the A-D pair, the

integers m and n are set to 0, 2 or 4 and to 0 or 2, respectively. The total term is zeroed when $\theta_{A\text{-}H\text{-}D}$ is less than 90° or when n is 2 and $\theta_{AA\text{-}A\text{-}H}$ is less than 90°. Two switch functions are used within the ranges from r_{on} to r_{off}, and θ_{on} to θ_{off}, respectively. In case $r^2_{AD} > r^2_{off}$, the switch function $sw(r^2_{AD})$ is set to zero; $sw(r_{AD}{}^2)$ equals 1 when $r^2_{AD} \leq r^2_{on}$. In between r_{on} and r_{off}, $sw(r^2_{AD})$ is used in order to get a smooth transition between the E_{hb} value at r_{on} and at distances larger than r_{off} [16]. The same holds for $\theta_{A\text{-}H\text{-}D}$. Default values have been used for r_{on}, r_{off}, θ_{on} and θ_{off}, i.e. 3.5 Å, 4 Å, 130° and 110°, respectively.

From Eq. 1, it is evident that in case n equals 2, E_{hb} will be most favourable for AA-A-H being 180° (i.e. $\cos^2(\theta_{AA\text{-}A\text{-}H}) = 1$). This theoretically (CHARMm) optimal value of 180° is not in agreement with the values determined from a thorough protein database search on H-bond geometries as reported by Ippolito et al. [18]. According to these authors, an optimal interaction with a carboxylate group occurs at 120° and not at 180°. Furthermore, these authors outline the differences between syn- and anti-interactions with carboxylate groups, thereby indicating that syn-interactions appear more in the plane of the carboxylate group and hence possess a more alkaline character than the anti-orientated interactions [18]. The optimal CHARMm value at 180° for $\theta_{AA\text{-}A\text{-}H}$ is thus only a very rough estimate. Further, the known dihedral dependence of H-bonds as demonstrated by H-bond clustering in the plane of carboxylates [18] is absent in Eq. 1, i.e. the AAA-AA-A...H or the alternative AAA-AA-A...D terms are not considered (with AA and AAA as acceptor antecedent and acceptor double antecedent, respectively). Furthermore, the applied CHARMm force field [15] only considers monopole–monopole interactions in the electrostatic potential function. Since it has been demonstrated that a correct H-bond geometry only results when higher order multipoles are included in the electrostatic potential [19,20], the CHARMm force field does consider the distance dependence of H-bonds properly, but describes the angle dependence inadequately. Although Eq. 1 does not yield a precise description of an H-bond, in view of the sizes of the molecular systems which are generally analysed with CHARMm, this equation provides a good compromise between physical accuracy and computational efficiency. However, if accurate energies are aimed at, which heavily rely on hydrogen-bonded interactions (such as the systems under investigation), this force field is not adequate. Therefore, an ab initio analysis (Fig. 1, step **11**) was performed.

Random sampling search (Fig. 1, step 8) The X-ray structure of histamine [21] was positioned in both receptor models (A and B) at two putative binding sites, one consisting of $Asp^{98}/Tyr^{182}/Asp^{186}$ and the other of $Asp^{98}/Asp^{186}/Thr^{190}$. The H-bonds involved in the three-point interaction were established with H-bond geometries as reported for X-ray data [18] by rotating the side chains of the amino acids involved. Subsequently, the random sampling search method [15] was applied to further optimize the position of histamine within its binding sites (step **8**). This specific method was chosen because of the considerable torsion space of the protein which had to be investigated, i.e. two torsion angles for each interacting residue. The hydroxyl torsion angle of Tyr^{182} was kept fixed in the phenolic plane during the search. The random sampling search method randomly changes all predefined torsion angles until a preset number of conformations is obtained. Each selected torsion angle was chosen to vary at most 120° during the search, because outside this range no H-bonds could be established between histamine and the putative binding sites. Histamine was allowed to be displaced from its starting position within the default rigid-body translation values (rigid-body torsion angle window of 15° and translation window of 0.5 Å [15]). Also the histamine side chain was allowed to adopt itself (two torsion angles with a 120° variation tolerance).

After each random change from the initial structure, an adopted basis Newton–Raphson minimization (default 400 steps) was automatically invoked [15]. During this minimization method, all geometric parameters were kept fixed, except for the torsion angles allowed to vary in the random sampling search method and the position of the histamine fragment with respect to the protein. In order to keep the histamine molecule in the vicinity of its putative binding site during the random sampling search and subsequent minimization procedures, distance constraints were applied to the hydrogen bond donor and acceptor atoms present in the three H-bonds responsible for the interaction between histamine and the histamine H_2 receptor. Default values (i.e. 25) were taken for both force constants K_{min} and K_{max} [15], which determine the steepness of the distance constraint potential function outside the range determined by the upper and lower bounds. These boundaries were set to 0.3 and 0.4 Å from the targeted distance, respectively. The targeted distances, i.e. the optimal distances, for the three H-bonds were preset to mean X-ray values as reported by Ippolito et al. [18] (cf. Fig. 6, Part I). Within the range defined by the upper and lower bounds, the constraint is satisfied, which determines the width of the square well of the CHARMm NOE constraint potential function [15]. In this way, a number of local minima (biased with predetermined H-bond distances) were created for the supermolecule.

Selection of low-energy conformations and CHARMm geometry optimization (Fig. 1, steps 9 and 10) The random sampling search procedure does not consider H-bonds explicitly [15]. Therefore, the four lowest energy conformations for each putative binding site emerging from the random sampling search were selected (Fig. 1, step **9**) and subsequently optimized in five phases with the explicit CHARMm H-bond function (Eq. 1) invoked (step **10**). Although the CHARMm force field can be

TABLE 2
RECEPTOR MODELLING RESULTS FOR THE PUTATIVE $Asp^{98}/Asp^{186}/Thr^{190}$ AND $Asp^{98}/Tyr^{182}/Asp^{186}$ BINDING SITES IN TWO MODELS FOR THE HISTAMINE H_2 RECEPTOR

Variable	Model A Asp^{186} / Thr^{190}	Model A Tyr^{182} / Asp^{186}	Model B Tyr^{182} / Asp^{186}
τ_1 [a]	−88.7°	−165.8°	65.6°
τ_2 [a]	144.1°	165.2°	167.6°
τ_3 [a]	51.9°	104.4°	67.8°
τ_4 [a]	177.5°	66.1°	104.7°
τ_5 [a]	–	4.1°	−14.0°
τ_6 [b]	−137.6°	−157.4°	169.4°
τ_7 [b]	−177.2°	178.3°	−177.8°
$\phi/\psi_{(182 \text{ or } 186)}$ [c]	−45.5/−50.3	−76.1/−57.4	−18.2/−43.4
$\phi/\psi_{(183 \text{ or } 187)}$ [c]	−49.2/−34.0	−69.4/−31.7	−83.6/18.0
$\phi/\psi_{(184 \text{ or } 188)}$ [c]	−82.6/−49.0	−63.0/−17.3	−54.3/−42.6
$\phi/\psi_{(185 \text{ or } 189)}$ [c]	−66.1/−40.4	−88.9/−49.5	−53.7/−66.6
$\phi/\psi_{(186 \text{ or } 190)}$ [c]	−91.3/17.5	−48.8/−46.9	−68.7/−25.7
$N...O_{(A)}^{98}$ [d]	3.80 Å	3.69 Å	3.00 Å
$N\text{-}H...O_{(A)}^{98}$ [d]	117.8°	154.6°	163.9°
$H...O_{(A)}^{98}\text{-}C_{(A)}^{98}$ [d]	138.5°	174.2°	160.1°
$N^{\pi}...O_{(A)}^{186}$	3.52 Å	2.98 Å	3.15 Å
$N^{\pi}\text{-}H^{\pi}...O_{(A)}^{186}$	135.2°	145.7°	149.0°
$H^{\pi}...O_{(A)}^{186}\text{-}C_{(A)}^{186}$	95.1°	160.7°	158.1°
$O_{(T)}^{182/190}...N^{\tau}$	3.56 Å	3.08 Å	3.23 Å
$O_{(T)}^{182/190}\text{-}H_{(T)}^{182/190}...N^{\tau}$	159.6°	167.8°	170.7°
$H_{(T)}^{182/190}...N^{\tau}\text{-}C_2$	89.1°	96.9°	103.0°
$E_{hb}(Asp^{98}\text{-His})$ [e]	−0.021	−1.100	−2.325
$E_{hb}(Asp^{186}\text{-His})$ [e]	−0.005	−1.438	−1.501
$E_{hb}(Tyr^{182}\text{-His})/E_{hb}(Thr^{190}\text{-His})$ [e]	−2.104	−3.448	−3.079
E_{inter} (6-31G*; CP) [f]	−13.62	−24.54	−25.79

[a] See Fig. 4 of Part I for the definition of τ_1–τ_5.

[b] τ_6 stands for the dihedral angle of the histamine side chain, measured as $N^{\pi}\text{-}C_5\text{-}C^{\beta}\text{-}C^{\alpha}$; the original X-ray value is −160.04 [21]; τ_7 stands for the dihedral angle of the histamine side chain, measured as $C_5\text{-}C^{\beta}\text{-}C^{\alpha}\text{-}N$; the original X-ray value is −170.61 [21].

[c] Backbone ϕ/ψ angles for the pentapeptide consisting of Tyr^{182}; Gly^{183}; Leu^{184}; Val^{185}; and Asp^{186} or for the pentapeptide containing Asp^{186}; Gly^{187}; Leu^{188}; Val^{189}; and Thr^{190}, respectively.

[d] Variables used in the CHARMm H-bond Eq. 1 for the H-bond between: the carboxylate of Asp^{98} (TM3) and the amino N from the histamine side chain; the proximal nitrogen atom of the histamine imidazole ring and Asp^{186}; and the tele-nitrogen atom of the histamine imidazole ring with Tyr^{182} or Thr^{190}.

[e] CHARMm H-bond energy values of the three H-bonds between histamine and the binding sites $Asp^{98}/Asp^{186}/Thr^{190}$ or $Asp^{98}/Tyr^{182}/Asp^{186}$ (in kcal/mol).

[f] Hartree–Fock basis set superposition error-corrected interaction energy in the 6-31G* basis (in kcal/mol).

biased towards accurate H-bond distances and angles by introducing dummy atoms and restraint forces as described in Part I, this would, however, require an in-depth study on the exact values of the force constants and upper and lower bounds to be used as indicated in the first part of this study. In view of the aforementioned uncertainties in the underlying receptor models, we omitted such a tedious study and confined ourselves to the less accurate CHARMm H-bond potentials.

As mentioned above, the geometry optimization consists of five stages (step **10**). At each stage of the procedure, optimizations were performed at default convergence criteria [15] with the steepest-descent (SD) method followed by the conjugate gradient (CG) method. The SD method applies first derivatives and rapidly improves a poor conformation. The CG method exhibits better convergence to a local minimum than the SD method, provided the molecular system has a reasonable conformation [22]. To simulate the interior of a protein, we employed a distance-dependent dielectric with a dielectric constant of 4 [16]. Cutoff values for the calculation of nonbonded and hydrogen-bonded interactions and the respective switch functions (cf. Eq. 1) were all taken at default values. Both nonbonded as well as hydrogen-bonded lists were updated every 50 cycles. In phase 1 of the optimization procedure, only the hydrogen atoms were optimized. In phase 2, only the backbone atoms were fixed, while all the other atomic positions were optimized. In phases 3 and 4, the flexibility of the backbone was gradually increased (harmonic forces of 100 and 10, respectively), whereas the N- and C-caps of the helices remained fixed. In phase 5, all the atomic positions were optimized, except for the helical ends, to maintain the relative orientations of the α-helices in the protein

models. In this final stage, the convergence criterion for the gradients in the CG method was lowered from 0.25 to 0.01 [15]. We kept the helical ends fixed during all stages of the minimization, in order to preserve the rationale underlying the construction of the original models: within Model A highly conserved residues point away from the lipid and a complete network of residues connected by correlated mutational behaviour was identified [1]; within Model B a conserved network of hydrogen bonds putatively involved in a ligand-activated transmembrane proton transfer was identified [3]. By fixing the relative orientation of the seven α-helices, these networks are assumed to be conserved throughout the minimization procedure.

Ab initio analysis (Fig. 1, step 11) The global minima resulting from the CHARMm optimizations on the two putative binding sites for Models A and B (step **10**) were further analysed with ab initio methods (step **11**, Fig. 1). For this purpose, the receptor models had to be reduced to the respective pentapeptides used as model systems in Part I (i.e. Y-G-G-G-D and D-G-G-G-T, respectively); histamine was reduced to 5-methylimidazole as in procedure step **5**, Section I (Fig. 1). The interaction energies calculated for 5-methylimidazole and the CHARMm-optimized pentapeptide can then be compared with the results from Section I, where the pentapeptide was restricted to standard ϕ/ψ angles. In this context, especially the ϕ/ψ angles of Gly^{183} and Gly^{187} are important. All ab initio calculations were done with the quantum chemical programme package GAMESS-UK [23–25] and were restricted to single-point energy calculations (Hartree–Fock (HF) 6-31G* basis set) and to the determination of the basis set superposition error-corrected interaction energy (using the counterpoise (CP) method; cf. Part I for further details on these computations). Thus, the complexes were directly extracted from the 3D protein Models A and B while all dihedral angles obtained after the CHARMm optimization were preserved (a.o. ϕ/ψ angles of the residues Gly^{183} and Gly^{187}).

Results and Discussion

The Asp^{98}/Asp^{186}/Thr^{190} binding site

Protein modelling results for the histamine H_2 receptor are depicted in Table 2. In Model B [3], it appeared to be impossible to obtain a reasonable histamine binding mode in between Asp^{98}, Asp^{186} and Thr^{190}. Despite the flexibility of the amino acid side chains, the shortest distance which could be obtained for the $N^{\tau}...O_{Thr}$ distance was approximately 5 Å. Also, within Model A, the Asp/Thr interaction resulted in inacceptable 'H-bonds'. The hydrogen bond between the positively charged amino group of histamine and Asp^{98} from TM3 appeared to be far from optimal: both the $N...O^{\delta\ 98}$ distance and the $N\text{-}H...O^{\delta\ 98}$ angle deviate largely from average X-ray values [18] (deviations of 0.9 Å and 60°, respectively). The valence angle for the donated proton with respect to $O^{\delta}\text{-}C^{\gamma}$ of Asp^{98} did lie close to its optimum of 120° and the interaction with the carboxylate appeared to be syn-orientated and 28° out of the plane (not shown in Table 2). Also the H-bond between the imidazole and Asp^{186} from TM5 is designated to be poor: an $N^{\pi}...O^{\delta\ 186}$ distance of 3.52 (0.6 Å deviation from the mean X-ray value), an $N^{\pi}\text{-}H^{\pi}...O^{\delta}$ angle of 135.2° (45° deviation), an $H^{\pi}...O^{\delta}\text{-}C^{\gamma}$ angle of 95.1° (25° deviation) and a very poor $H^{\pi}...O^{\delta}\text{-}C^{\gamma}\text{-}C^{\beta}$ value of 101.2°. The interaction between the imidazole and Asp^{186} can thus be seen as a 'syn'-interaction being 80° out of the carboxylate plane. The H-bond between the imidazole and Thr^{190} is acceptable: the $O_{(T)}...N^{\tau}$ distance is rather large (3.56 Å), but the $O_{(T)}\text{-}H_{(T)}...N^{\tau}$ angle deviates only 20° from the optimal (180°). The $H_{(T)}...N^{\tau}\text{-}C_2$ angle equals 98.1° and deviates about 30° from the optimal (i.e. 126°), whereas the proton is donated within 25° of the imidazole plane. The CHARMm H-bond energy values (E_{hb} in Table 2) confirm that only the latter H-bond yields a considerable amount of energy (–2.1 kcal/mol).

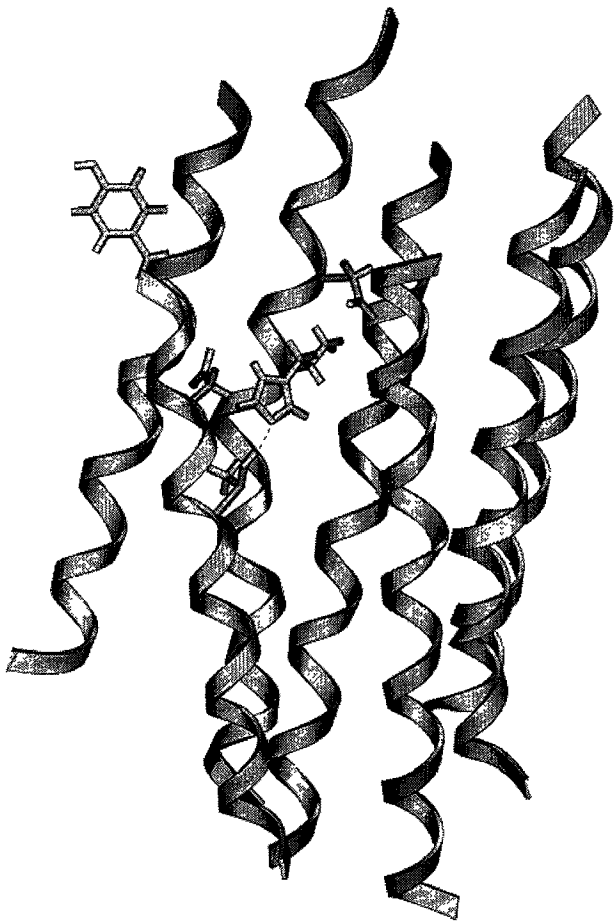

Fig. 2. Binding of histamine within the putative Asp^{98} (TM3) / Asp^{186} (TM5) / Thr^{190} (TM5) agonistic binding site in Model A [2] for the histamine H_2 receptor. Only a modest H-bond between histamine and Thr^{190} is observed. The α-helical backbone structure around Thr^{190} is disturbed. The picture was made with SETOR, v. 4.13.4 (University of British Columbia [32]).

Visualization of Model A (Fig. 2) clearly reveals that Asp^{186} is pointing towards the extracellular surface, instead of interacting with histamine, while the H-bond between the imidazole and Thr^{190} is the only acceptable one. Table 2 reveals that histamine binds to this binding site in an extended (trans–trans) conformation (Table 2, dihedrals τ_6 and τ_7). Considering the $Asp^{98}/Asp^{186}/Thr^{190}$ binding site within Model A, the residues 186–190 all have ϕ/ψ backbone angles which fall within the range allowed for an α-helical state [26], however, except for Thr^{190} (Table 2). For this residue, ϕ/ψ angles are observed (–91.3/17.5) which largely deviate from standard α-helical values (–57°/–47° [27]). In the model as provided by the authors [2], Thr^{190} displayed correct α-helical behaviour. In our final optimized Model A, a right-handed bridge conformation [26] is, however, observed for Thr^{190}. The disruption of the α-helical structure induced by histamine binding to this Asp/Thr site supports our earlier conclusions that histamine will preferably not bind to this site.

The $Asp^{98}/Tyr^{182}/Asp^{186}$ binding site

Within the putative $Asp^{98}/Tyr^{182}/Asp^{186}$ binding site, a three-point interaction with histamine can be established in both protein Models A and B. In Model B, optimal H-bonds are observed (Fig. 4). In Model A (Fig. 3), the amino nitrogen of the histamine side chain is at a rather large distance from Asp^{98} (3.98 Å compared to the average X-ray value of 2.9 Å [18]). All other variables are close to the observed X-ray values (see Table 2). In both models, Asp^{98} accepts a proton from the histamine side chain in the plane of the carboxylate (syn-orientated). The H-bond between the imidazole ring system (N^{π}-H) and Asp^{186} is seen to occur syn-orientated at angles of 60° and 42° out of the plane of the carboxylate for Models A and B, respectively. The H-bond between N^{τ} and Tyr^{182} occurs at angles of 40° and 2° out of the imidazole plane in Models A and B, respectively. Table 2 reveals that histamine binds to this binding site in an extended (trans–trans) conformation (Table 2, dihedrals τ_6 and τ_7). The CHARMm H-bond energies (E_{hb}, Table 2) show that all three H-bonds contribute at least 1 kcal/mol to histamine binding at the $Asp^{98}/Tyr^{182}/Asp^{186}$ binding site in both Models A and B.

A final inspection of the ϕ/ψ angles of the amino acids 182–186 reveals that in Model A the largest deviation from standard α-helical ϕ/ψ angles is observed for the ψ angle of Leu^{184} (30°). Thus, histamine binding does not disrupt the α-helical structure in Model A. However, in Model B, histamine binding induces a right-handed bridge conformation in Gly^{183}. Since Gly residues are highly flexible and Gly^{183} also lies close to the TM5 N-cap, this distortion is probably more acceptable than the one at position 190 observed for the Asp^{186}/Thr^{190} binding site.

In summary, both Models A and B can accommodate histamine at the $Asp^{98}/Tyr^{182}/Asp^{186}$ binding site through a three-point H-bond interaction. Within Model B, hydrogen bonds are optimal, and within Model A the binding site at TM5 becomes less distorted from an α-helical structure. No decisive conclusion in favour of one of the two employed models can therefore be drawn yet.

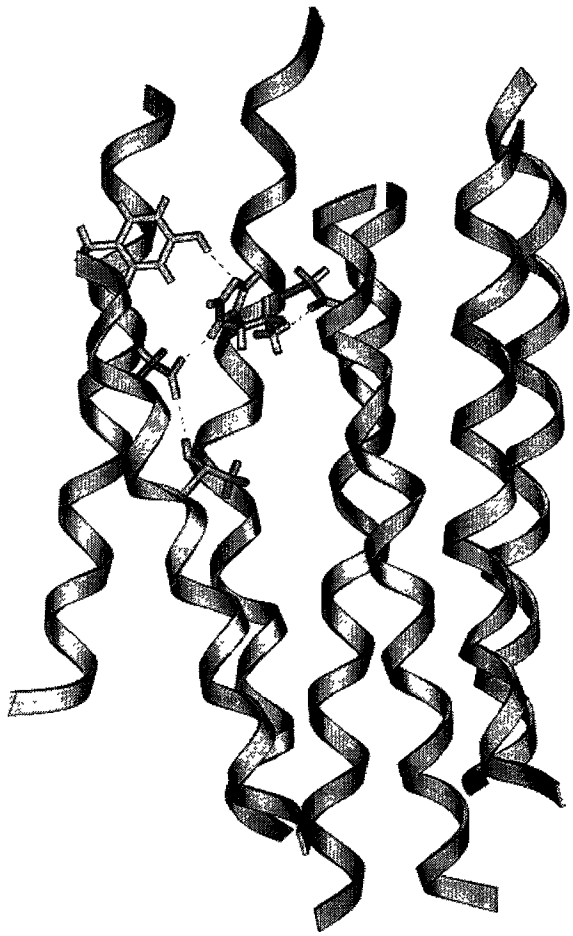

Fig. 3. Binding of histamine via three H-bonds within the putative Asp^{98} (TM3) / Tyr^{182} (TM5) / Asp^{186} (TM5) agonistic binding site in Model A [2] for the histamine H_2 receptor. The H-bond between the histamine side chain and Asp^{98} is not optimal (see text). Thr^{190} is seen to form an H-bond with Asp^{186}. The picture was made with SETOR [32].

A comparison between oligopeptide (Part I) and protein model (Part II) results

Absolute HF (6-31G*) CP interaction energies for the receptor models (Table 2, last row) are found to be lower than those for the oligopeptide model system described in Part I (Table 4). This is not surprising, since the backbone atoms of the receptor models were fully optimized (except for the helical ends). A comparison of Table 4 (Section I, Part I) and Table 2 (this section) reveals that especially the Tyr/Asp interaction benefits from this additional flexibility: the interaction energy (E_{inter}) increases from approximately –20 kcal/mol to almost –26 kcal/mol (protein Model B). The Asp/Thr interaction benefits only in a modest way, i.e. –13.1 versus –13.6 kcal/mol.

For the $Asp^{98}/Tyr^{182}/Asp^{186}$ histamine binding in Model A (Fig. 3), Thr^{190} was found to form an H-bond with Asp^{186}. The average C-S-donor/acceptor bond length for a Cys residue is 3.5 (± 0.1) Å, whereas the comparable length for Thr is 2.9 (±0.2) Å [18]. In addition, their pK_a values differ significantly, being approximately 8 and 13, respectively (cf. Part I and Ref. 18). Therefore, the reported mutation Thr^{190} to Cys^{190} [9] could result in a strong H-bond between Asp^{186} and Cys^{190}, which in turn could interfere with agonist binding. In Model B, Thr^{190} was seen to form an H-bond with the backbone of TM5. This observation is in accordance with our earlier observations that the global minimum for Thr^{190} is achieved by H-bond formation with the α-helical structure (Fig. 9, Part I). Hence, the monitored effects of mutating Thr^{190} on histamine binding and receptor activation [9] could indeed be indirect: (i) via destabilization of the α-helix resulting in a different relative orientation of amino acids; or (ii) interference with the alleged H-bond between the agonist and Asp^{186}.

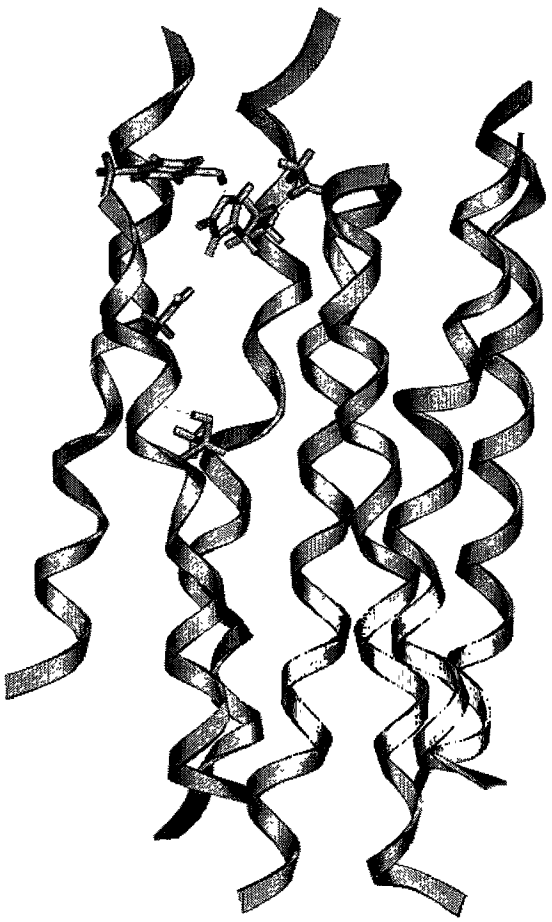

Fig. 4. Binding of histamine via three H-bonds within the putative Asp^{98} (TM3) / Tyr^{182} (TM5) / Asp^{186} (TM5) agonistic binding site in Model B [3] for the histamine H_2 receptor. Thr^{190} is observed to form an H-bond with the backbone, thereby stabilizing the α-helical configuration of TM5. The high flexibility of Gly^{183} leads to a deviation of the α-helical structure of TM5 near the N-cap (see text). The picture was made with SETOR [32].

Substituted histamine analogues

Substitution of the imidazole ring system of histamine results, in many cases, in a sharp decrease in H_2 agonistic activity. However, 4/5-methyl- (cf. compound **3**, Table 1) and 4/5-ethylhistamine show only a slight decrease in activity [10,11,28]. We have therefore checked whether this substitution is allowed, and, indeed, in both Models A and B (assuming a similar binding mode of histamine and its substituted analogues) a methyl or ethyl substitution next to the 2-aminoethyl side chain of histamine is sterically allowed for both the $Asp^{98}/Tyr^{182}/Asp^{186}$ and $Asp^{98}/Asp^{186}/Thr^{190}$ binding sites. Furthermore, several known histamine H_2 receptor agonists are substituted with either an amino or a methyl group at the 2-position of the heterocycle. Examples of substituted histamine analogues, which are weakly active at the histamine H_2 receptor, are given in Table 1 and in e.g. Refs. 10 and 11. Therefore, we also verified whether this substitution is tolerated within the binding sites under investigation assuming that the substituted histamine analogues bind in the same manner as histamine itself.

The binding of 2-methylhistamine (compound **2**, Table 1) at the $Asp^{98}/Asp^{186}/Thr^{190}$ binding site within Model A resulted in two collisions: one between the methyl substituent and the C^{γ} of Asp^{186} and the other between the methyl and O^{δ} of Asp^{186} (distances of 2.49 and 2.32 Å, respectively). Amino substitution at the 2-position (compound **4**, Table 1) resulted in similar collisions. Additional H-bonds between the 2-amino group and the carboxylate of Asp^{186} were not observed.

Within Model A and the $Asp^{98}/Tyr^{182}/Asp^{186}$ binding site, no unfavourable interactions were observed for compounds **2** and **4** (Table 1), whereas an additional H-bond between the 2-amino group and Asp^{186} was registered ($N...O^{\delta\ 186}$ of 3.2 Å, $N-H...O^{\delta\ 186}$ of 148.7° and $H...O^{\delta\ 186}-C^{\gamma\ 186}$ of 108.3°). Within Model B, no 'bumps' occurred between the 2-methyl substituent and the Tyr^{182}/Asp^{186} binding site, whereas the 2-amino substituent could potentially form an additional H-bond with Asp^{186} ($N-O^{\delta\ 186}$ of 4.43 Å, $N-H...O^{\delta\ 186}$ of 147.9° and $H...O^{\delta\ 186}-C^{\gamma\ 186}$ of 96.7°). An additional CHARMm optimization revealed that such an H-bond could indeed be formed. Hence, the two investigated 2-substituted histamine analogues confirm the earlier conclusions regarding the most optimal binding site, i.e. the Tyr/Asp couple, but hardly differentiate between protein Models A and B.

Conclusions

Receptor models [1–3] for the transmembrane domains of the histamine H_2 receptor reveal that the postulated three-point interaction for histamine with the H_2 receptor [9–14] cannot be established simultaneously with Asp^{98}, Asp^{186} and Thr^{190}. This can only be achieved within the alternative binding site consisting of Asp^{98}, Tyr^{182} and

Asp^{186}, and only this alternative binding site permits amino or methyl substitution at the 2-position of the imidazole ring system. Furthermore, substitution by either a methyl or an ethyl group next to the histamine 2-aminoethyl side chain is sterically allowed. Hence, our conclusion from Part I of this study suggesting that the agonistic binding site of the histamine H_2 receptor consists of Asp^{98}, Tyr^{182} and Asp^{186} has also been confirmed in two protein models. Moreover, it is noted that histamine has its side chain in an extended (trans–trans) conformation as predicted by Eriks et al. [11] and Sippl et al. [14].

Histamine recognition and the α-helical dipole moment

The dipole moment of the fifth transmembrane α-helix of the histamine H_2 receptor is directed from the cytoplasm towards the periplasma (the dipole is taken from δ^- to δ^+). Within the Tyr/Asp binding site, the alkaline nitrogen of histamine (N^τ) is at the periplasmic side of the fifth α-helix. Hence, the imidazole moiety couples with the α-helical dipole moment in an energetically favourable manner. Within the Asp/Thr binding site, the imidazole ring system does not bind in the direction of the α-helical dipole moment (now the N-H is at the periplasmic side and the basic =N- faces the cytoplasm). Correct coupling with the dipole vector of an α-helix can contribute to a better interaction [29], favouring the Tyr^{182}/Asp^{186} interaction. It is not unlikely that the recognition of histamine by the histamine H_2 receptor is partially guided by a complementary coupling between the dipole moments of the receptor and the electrical field of the ligand. In that case, histamine is directed with its imidazole ring in such a way that the Tyr^{182}/Asp^{186} coupling is facilitated. The Asp^{186}/Thr^{190} interaction clearly lacks these additional coupling possibilities.

Additional evidence from mutation studies on the histamine H_1 receptor

From the mutation studies reported by Gantz et al. [9], it has become clear that Asp^{98} from the third transmembrane α-helix of the histamine H_2 receptor plays a crucial role in agonist binding and subsequent receptor activation. Mutations at the fifth transmembrane domain of this G-protein-coupled receptor appear to influence the pharmacological characteristics induced by histamine exposure. Therefore, it seems likely that histamine interacts with the fifth α-helix, albeit with an alternative couple: Tyr^{182} and Asp^{186}. Thr^{190} is found to interact with the receptor backbone (cf. Figs. 4 (this part) and 9 (Part I)), and is therefore suggested to have an indirect effect on histamine binding.

Additional evidence for the involvement of Tyr^{182} in H_2 agonist binding and receptor activation can possibly be deduced from the homology between the histamine H_1 and H_2 receptors. Molecular modelling studies in combination with mutation experiments on the histamine H_1 receptor have been reported [30,31]: also for the histamine H_1 receptor it appears to be impossible for histamine to bind to the earlier alleged histamine H_1 receptor TM5 residues Thr^{203}/Asn^{207} (which correspond to the Asp^{186}/Thr^{190} couple in the histamine H_2 receptor). It has been demonstrated that a lysine residue (Lys^{200}), positioned very close to the periplasma of TM5, is involved in histamine-induced H_1 receptor activation [30,31, and references cited therein]. This lysine residue corresponds to position 183 in the histamine H_2 receptor, which is next to the putative proton donor Tyr^{182}.

Future perspectives

Within the resulting histamine H_2 receptor models, the first step in the activation model (i.e. a proton transfer from Tyr^{182} towards the tele-nitrogen of the histamine imidazole; cf. Fig. 2, Part I) can be studied. The binding energies of a series of known histamine H_2 receptor agonists as well as the energetics of the mentioned proton shift [10,11] can be determined in order to explain the observed differences between the pK_d and pD_2 values (in other words, differences in receptor reserves) for a series of substituted imidazoles and thiazoles [11]. For this purpose, a pentapeptide can be used in ab initio calculations.

Timms et al. [3] have used the dicationic form of histamine as the active species in their proton pump model for the histamine H_2 receptor. However, Eriks et al. [11] have experimentally shown that histamine is biologically active in its monocationic form at the histamine H_2 receptor. Our model can thus be integrated with Timms's model: after proton donation from Tyr^{182} towards histamine, the agonist is present as dication, which is precisely the premise for Timms et al. [3] to develop their pump theory.

Molecular modelling in combination with molecular biology techniques appears to be useful in elucidating receptor binding and activation processes, which is illustrated by the aforementioned findings in relation to both the histamine H_1 and H_2 receptors [9,30,31]. Furthermore, the combined application of these techniques revealed the existence of at least two (partially) different agonistic binding sites at the histamine H_1 receptor. Mutation studies concerning the histamine H_2 receptor residue Tyr^{182} have been initiated in our laboratories in order to test our theoretical predictions on its merits. These studies will also elucidate whether or not our assumption is valid that the substituted histamine analogues depicted in Table 1 and/or thiazole/selenazole-containing compounds (cf. Fig. 2, Part I) indeed bind to the same receptor site as histamine itself.

Acknowledgements

We gratefully acknowledge Dr. Robin H. Davies

(Welsh School of Pharmacy, Cardiff) for providing us with the 3D coordinates of his β_1 adrenergic receptor model and Dr. Gert Vriend (EMBL, Heidelberg) for making his 'imaginations' public domain. The investigations were supported in part (P.H.J.N.) by the Netherlands Foundation for Chemical Research (SON) with financial aid from the Netherlands Organization for Scientific Research (NWO). We express our gratitude to the Dutch National Computer Facilities (NCF) for providing us with a very generous grant of supercomputer time on a Cray C98.

References

1 Oliveira, L., Paiva, A.M.C. and Vriend, G., J. Comput.-Aided Mol. Design, 7 (1993) 649.
2 Vriend, G., 'Gert Vriend's imagination', a 3D model of the histamine H_2 receptor is available from the TM7 file server
3 Timms, D., Wilkinson, A.J., Kelly, D.R., Broadley, K.J. and Davies, R.H., Recept. Channels, 2 (1994) 107.
4 Hoflack, J., Trumpp-Kallmeyer, S. and Hibert, M., Trends Pharmacol. Sci., 15 (1994) 7.
5 Schertler, G.F.X., Villa, C. and Henderson, R., Nature, 362 (1993) 770.
6 Baldwin, J.M., EMBO J., 12 (1993) 1693.
7 Unger, V.M. and Schertler, G.F.X., Biophys. J., 68 (1995) 1776.
8 Gantz, I., Munzert, G., Tashiro, T., Schäffer, M., Wang, L., DelValle, J. and Yamada, T., Biochem. Biophys. Res. Commun., 178 (1991) 1386.
9 Gantz, I., DelValle, J., Wang, L., Tashiro, T., Munzert, G., Guo, Y.-J., Konda, Y. and Yamada, T., J. Biol. Chem., 267 (1992) 20840.
10 Nederkoorn, P.H.J., Vernooijs, P., Donné-Op den Kelder, G.M., Baerends, E.J. and Timmerman, H., J. Mol. Graph., 12 (1994) 242.
11 Eriks, J.C., Van der Goot, H. and Timmerman, H., Mol. Pharmacol., 44 (1993) 886.
12 Weinstein, H., Mazurek, A.P., Osman, R. and Topiol, S., Mol. Pharmacol., 29 (1986) 28.
13 Nagy, P.I., Durant, G.J., Hoss, W.P. and Smith, D.A., J. Am. Chem. Soc., 116 (1994) 4898.
14 Sippl, W., Stark, H. and Höltje, H.-D., Quant. Struct.–Act. Relatsh., 14 (1995) 121.
15 QUANTA/CHARMm, v. 4.0, Simulation, Search, and Analysis, and CHARMm dictionary, Molecular Simulations Inc., Burlington, MA, U.S.A.
16 Brooks, B.R., Bruccoleri, R.E., Olafson, B.D., States, D.J., Swaminathan, S. and Karplus, M., J. Comput. Chem., 4 (1983) 187.
17 Chem-X Reference Guide, Chemical Design Ltd., Oxon, U.K., July 1994.
18 Ippolito, J.A., Alexander, R.S. and Christianson, D.W., J. Biol. Chem., 215 (1990) 457.
19 Van Duijneveldt-Van de Rijdt, J.G.C.M. and Van Duijneveldt, F.B., J. Am. Chem. Soc., 93 (1971) 5644.
20 Smit, P.H., Derissen, J.L. and Van Duijneveldt, F.B., J. Chem. Phys., 67 (1977) 274.
21 Cambridge Structural Database; Refcode hisahc10: Bonnet, J.J., Jeannin, Y. and Laaouini, M., Bull. Soc. Fr. Miner. Cri., 98 (1975) 208.
22 Schlegel, H.B., In Lawley, K.P. (Ed.) Ab Initio Methods in Quantum Chemistry – I, Wiley, New York, NY, U.S.A., 1987, pp. 249–286.
23 GAMESS-UK is a package of ab initio programmes written by Guest, M.F., Van Lenthe, J.H., Kendrick, J., Schoeffel, K., Sherwood, P. and Harrison, R.J., with contributions from Amos, R.D., Buenker, R.J., Dupuis, M., Handy, N.C., Hillier, I.H., Knowles, P.J., Bonacic-Koutecky, V., Von Niessen, W., Saunders, V.R. and Stone, A.J. The package is derived from the original GAMESS code, see Ref. 24.
24 Dupuis, M., Spangler, D. and Wendoloski, J., GAMESS, Natural Resource of Computational Chemistry Software Catalog, Vol. 1, Program No. QG01, 1980.
25 Guest, M.F., Fantucci, P., Harrison, R.J., Kendrick, J., Van Lenthe, J.H., Schoeffel, K. and Sherwood, P., GAMESS-UK User's Guide and Reference Manual, CFS Ltd., Daresbury Laboratory, Daresbury, U.K., 1993.
26 Némethy, G. and Scheraga, H.A., Q. Rev. Biophys., 10 (1977) 239.
27 Darbey, N.J. and Creighton, T.E., In Rickwood, D. (Ed.) Protein Structure, IRL Press, Oxford, U.K., 1993, pp. 1–22.
28 Ganellin, C.R., In Ganellin, C.R. and Parsons, M.E. (Eds.) Pharmacology of Histamine Receptors, Wright, Bristol, U.K., 1982, pp. 10–102.
29 Hol, W.G.J., Prog. Biophys. Mol. Biol., 45 (1985) 149.
30 Ter Laak, A.M., Leurs, R., Smit, M.J., Nederkoorn, P.H.J., Timmerman, H. and Donné-Op den Kelder, G.M., J. Comput.-Aided Mol. Design, 9 (1995) 319.
31 Leurs, R., Smit, M.J., Meeder, R., Ter Laak, A.M. and Timmerman, H., Biochem. Biophys. Res. Commun., 214 (1995) 110.
32 Evans, S.V., J. Mol. Graph., 11 (1993) 134.